Review of general resistive wall boundary condition for NIMROD

Andrea Montgomery
University of Wisconsin – Madison

with C. C. Hegna, C. R. Sovinec (UW Madison),
S. E. Kruger (Tech-X Corp), and S. A. Sabbagh (Columbia U)

Nimrod Team Meeting – August 13th, 2013 – Boulder, CO

Motivation

- An external wall of finite resistivity plays a major roll in the stability of tokamak devices via a variety of mechanisms:
  - resistive wall mode (RWM): a slow-growing extension of the external kink mode
  - vertical displacement events allowed by resistive wall
  - leaking of external error-fields through the wall, allowing externally driven magnetic islands
  - eddy currents driven in wall which produce a torque on plasma structures, thereby affecting plasma rotation (i.e. through island locking to the wall)
  - resistive wall can be a component of a feedback control scheme
- These mechanisms can be more thoroughly studying by simulating them in an extended MHD code such as NIMROD.

General resistive wall boundary condition uses numerically determined vacuum field

- Given the location of points on the wall, a Green's function solver (A. Pletzer's GRIN code) determines the vacuum response matrix M, such that, for wall locations w:

$$\chi^n(w) = \sum_{w'} M^n(w,w')B^n_{norm}(w')$$

$$\vec{B}^n_{vac} = \nabla\chi^n$$

- This field is then matched across the resistive wall with the perturbed plasma magnetic field calculated by NIMROD to find the n Fourier component of the electric field in the wall.

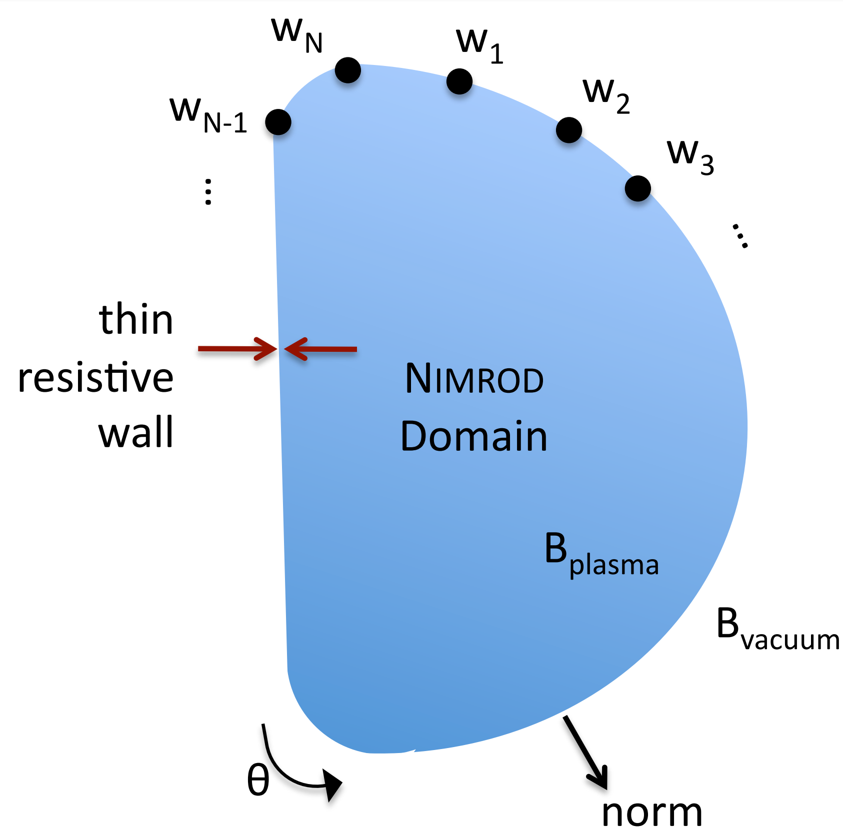

$$\hat{\mathbf{r}}\cdot\left[\mathbf{B}_{vac} - \mathbf{B}_{plasma}\right] = 0$$

$$\hat{\mathbf{r}}\times\left[\mathbf{B}_{vac} - \mathbf{B}_{plasma}\right] = \mu_0\mathbf{K} = \frac{\mu_0\delta_{wall}}{\eta_{wall}}\mathbf{E}_T$$

Surface electric field dependent on perturbed plasma fields and χ and its derivatives

- Symmetric toroidal geometry couples poloidal m numbers, but leaves toroidal n numbers decoupled; the general resistive wall boundary condition is consistent with this.

$$\vec{E}^{\,n} = v_w \hat{n} \times \left(\nabla \chi^n - \vec{B}^n_{plasma} \right)$$

$$\vec{E}^{\,n} = v_w \left[\left(\frac{-in}{R} \chi + B_{p\phi} \right) \hat{\theta} + \left(\nabla_\theta \chi - B_{p\theta} \right) \hat{\phi} \right]$$

$$v_w \equiv \frac{\eta_{wall}}{\mu_0 \delta_{wall}} \qquad \tau_w \equiv \frac{r_{wall}}{v_{wall}}$$

- Here, θ indicates the direction tangential to the surface in the R-Z plane.
- No-slip velocity boundary conditions are imposed. $\vec{v} = 0$

A second boundary condition on B_{norm} is required in NIMROD

- An additional boundary condition specifying B_{norm} at the next time step is required because NIMROD uses $\nabla \cdot \vec{B}$ cleaning instead of enforcing $\nabla \cdot \vec{B} = 0$.
- A direct calculation of ΔB_{norm} from Faraday's law would require second derivatives of χ in the poloidal direction (in the R-Z plane,) which are discontinuous for the numerical expansion used.
- Instead, we use test functions (α_i) to create a weak-form surface integral that only requires known derivatives of the test functions.

$$\Delta B_{norm} = -\Delta t \left(\nabla \times \vec{E} \right)_n$$

$$\oint_S \alpha \frac{\Delta B_{norm}^n}{\Delta t} dS = -\oint_S \left[\nabla \cdot \left(\vec{E}^n \times \alpha \hat{n} \right) + \vec{E}^n \cdot \nabla \times \left(\alpha \hat{n} \right) - \frac{in\alpha}{R} E_\theta^n \right] dS$$

Boundary condition on B_{norm} uses the weak form of Faraday's law

- The test functions (α_i) are the same as the interpolating functions by which each field is represented at nodes within each cell.

$$\oint_S \alpha_i \alpha_j w_j \Delta B^n_{norm,j} dS = \Delta t \oint_S \left[\alpha_j w_j E^n_{\phi,j} \nabla_\theta \alpha_i + \frac{in}{R} \alpha_i \alpha_j w_j E^n_{\theta,j} \right]$$

- Choosing Gauss-Lobatto-Legendre (GLL) spacing of nodes **and** Lobatto integration for the edge makes the mass matrix on the LHS diagonal, so that the inversion needed to solve for B_{norm} is trivial, and, more importantly, local.
- We still want to use Gaussian integration in the interior, so the ability to specify different integration schemes for the bulk and the edge has been added.
- As with the second boundary condition for the periodic cylinder, this boundary condition is applied after the matrix solve.

GLL spacing and Lobatto integration allow for simple mass-matrix inversion

- Positions of interior nodes (with vertices at 0 and 1) are either uniform (default) or Gauss-Lobatto-Legendre (gll, used here)
- Choice of integration scheme (default: Gaussian, here: Lobatto) sets gaussian quadrature points. For Lobatto integration, they are co-located with the gll-spaced nodes and vertices

Interpolating functions, α_i shown for p_d=3

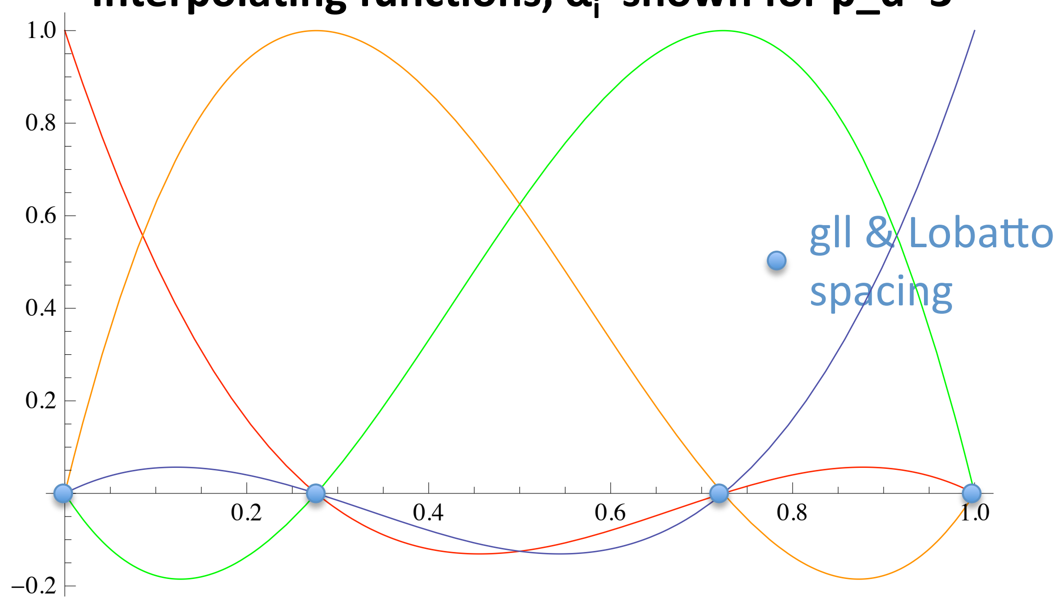

$$\oint_S \alpha_i \alpha_j w_j \Delta B^n_{norm,j} dS = \Delta t \oint_S \left[\alpha_j w_j E^n_{\phi,j} \nabla_\theta \alpha_i + \frac{in}{R} \alpha_i \alpha_j w_j E^n_{\theta,j} \right]$$

Original cylindrical boundary conditions and simple equilibrium are used to test new code

- A simple analytic equilibrium modified for use in NIMROD:
  - top-hat current profile modeled as tanh current profile
  - vacuum region between plasma and wall modeled as sparse, resistive region
- Perturb this equilibrium with a B_r eigenfunction proportional to $\cos(2\theta-\phi)$ that has $B_r \neq 0$ at the wall.
- This equilibrium is unstable to a m=2,n=1 RW mode (similar to an external kink.)

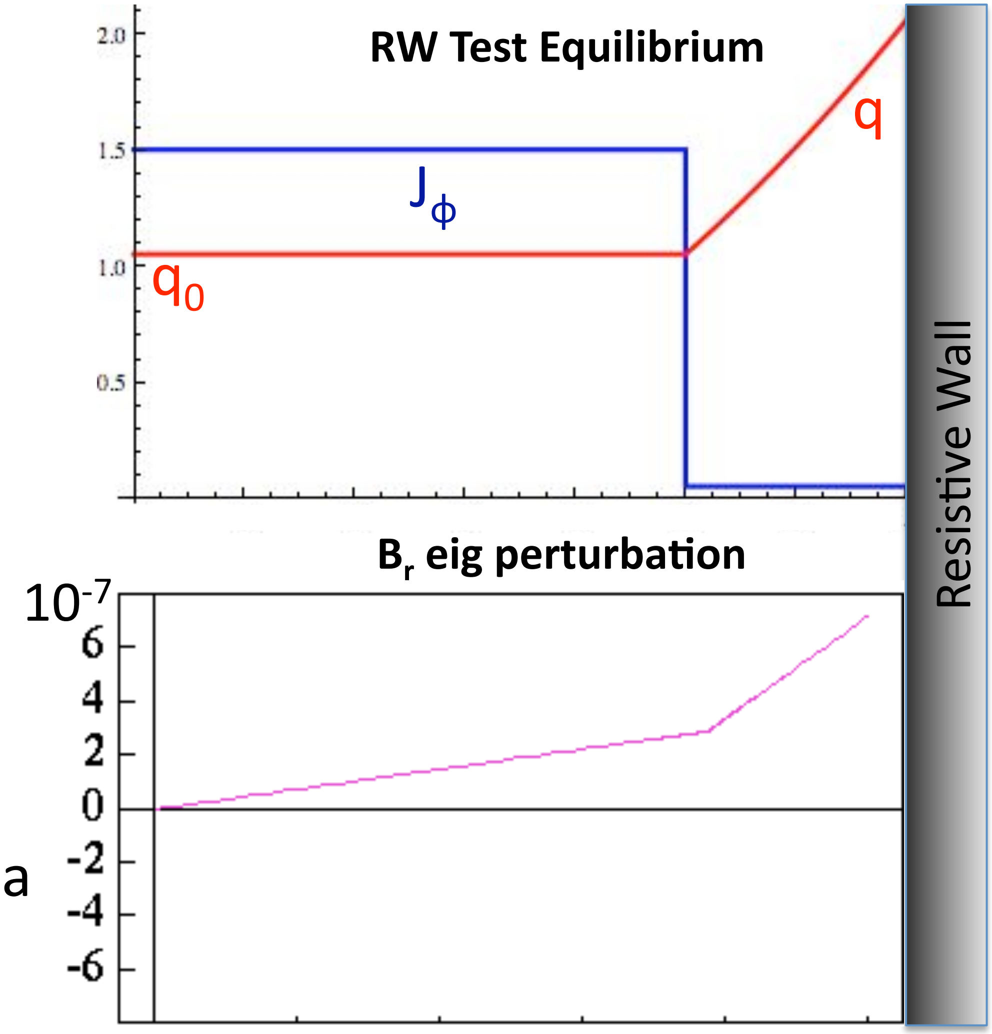

The vacuum response matrix for a periodic cylinder is used to test new boundary condition

- Using a Green's function method, we can derive the vacuum response matrices for each n in a periodic cylinder:

$$\chi = \left(\overleftrightarrow{I} + \overleftrightarrow{P}\right)^{-1} \overleftrightarrow{Q} B_{norm}$$

$$P_{ij} = 4\pi^2 k r_w \left[I_0{}' K_0 + 2\sum_{m=1}^{\infty} I_m{}' K_m \cos\left(m\left(\theta_i - \theta_j\right)\right)\right]$$

$$Q_{ij} = 4\pi^2 r_w \left[I_0 K_0 + 2\sum_{m=1}^{\infty} I_m K_m \cos\left(m\left(\theta_i - \theta_j\right)\right)\right]$$

- This vacuum response matrix is for n≠0 since the n=0 vacuum fields cancel out plasma equilibrium fields.
- Inverse is found using an LU decomposition, and backsubstituting columns of Q to eliminate the need for matrix multiplication.
- These matrices are real, indicating that there is no phase shift between the plasma fields and the vacuum fields.

Computed growth rate is within 2% of the analytic rate as wall location is varied

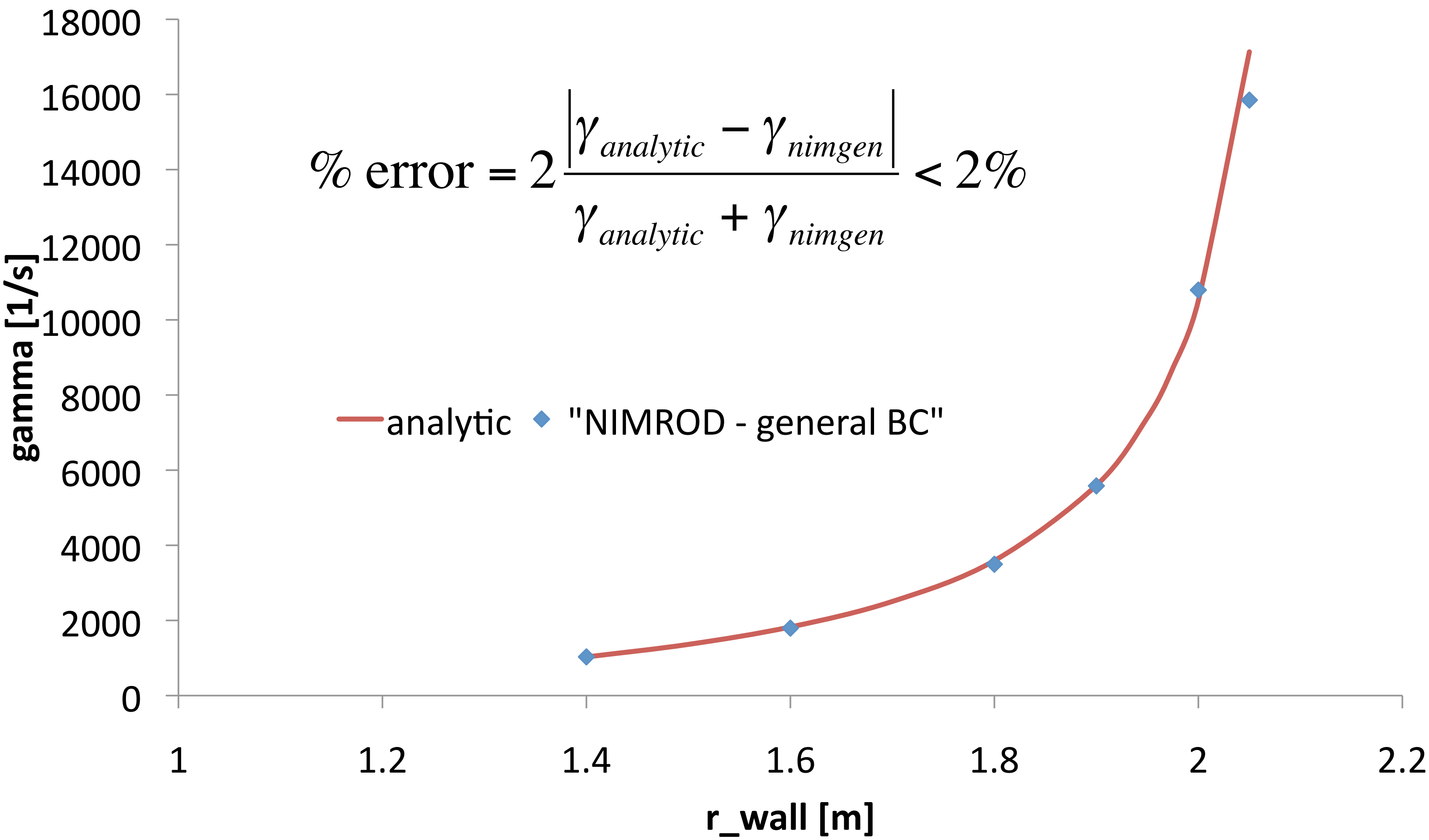

Computed growth rate is within 3% of the analytic rate as wall resistivity is varied

$$\%\ \text{error} = 2\frac{\left|\gamma_{analytic} - \gamma_{nimgen}\right|}{\gamma_{analytic} + \gamma_{nimgen}} < 3\%$$

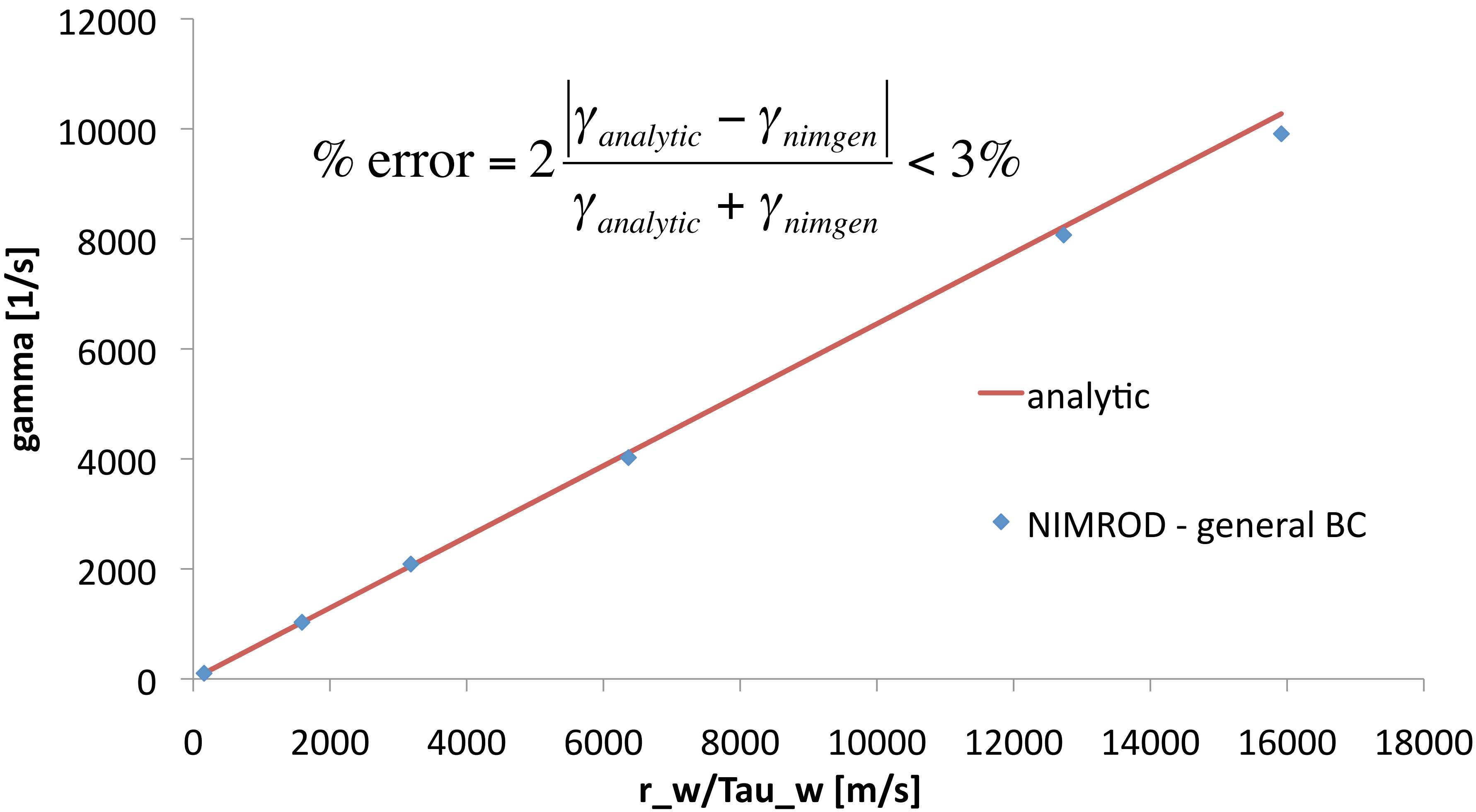

Magnetic field profiles from new RW boundary condition match original test profiles

perturbed B_normal perturbed B_poloidal

Per_cyl BC

General BC

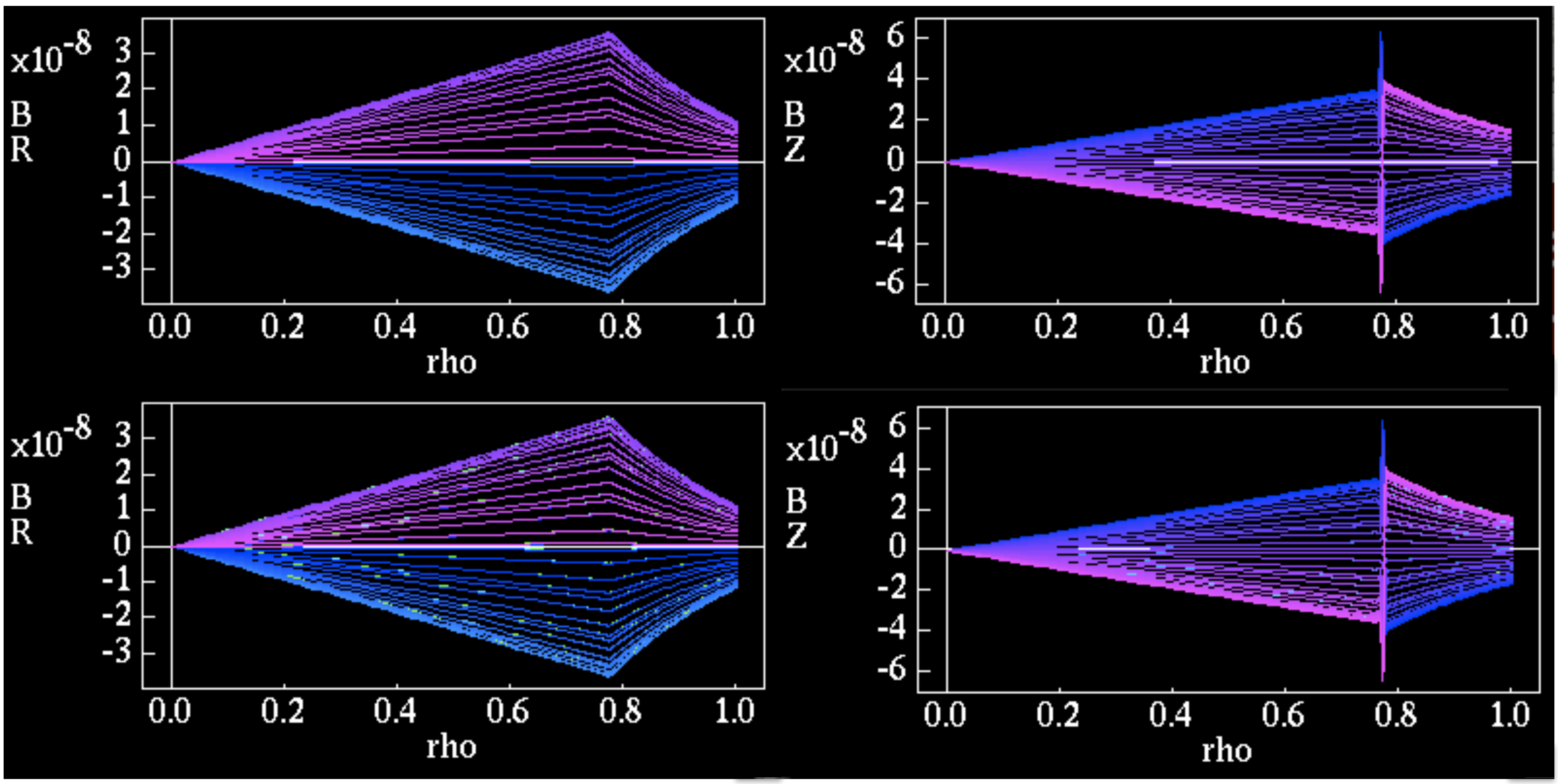

- Magnetic field profiles match analytic predictions for a m=2, n=1 kink-like resistive wall mode, and have $B_r \neq 0$ at the wall.

Velocity profiles from new RW boundary condition match original test profiles

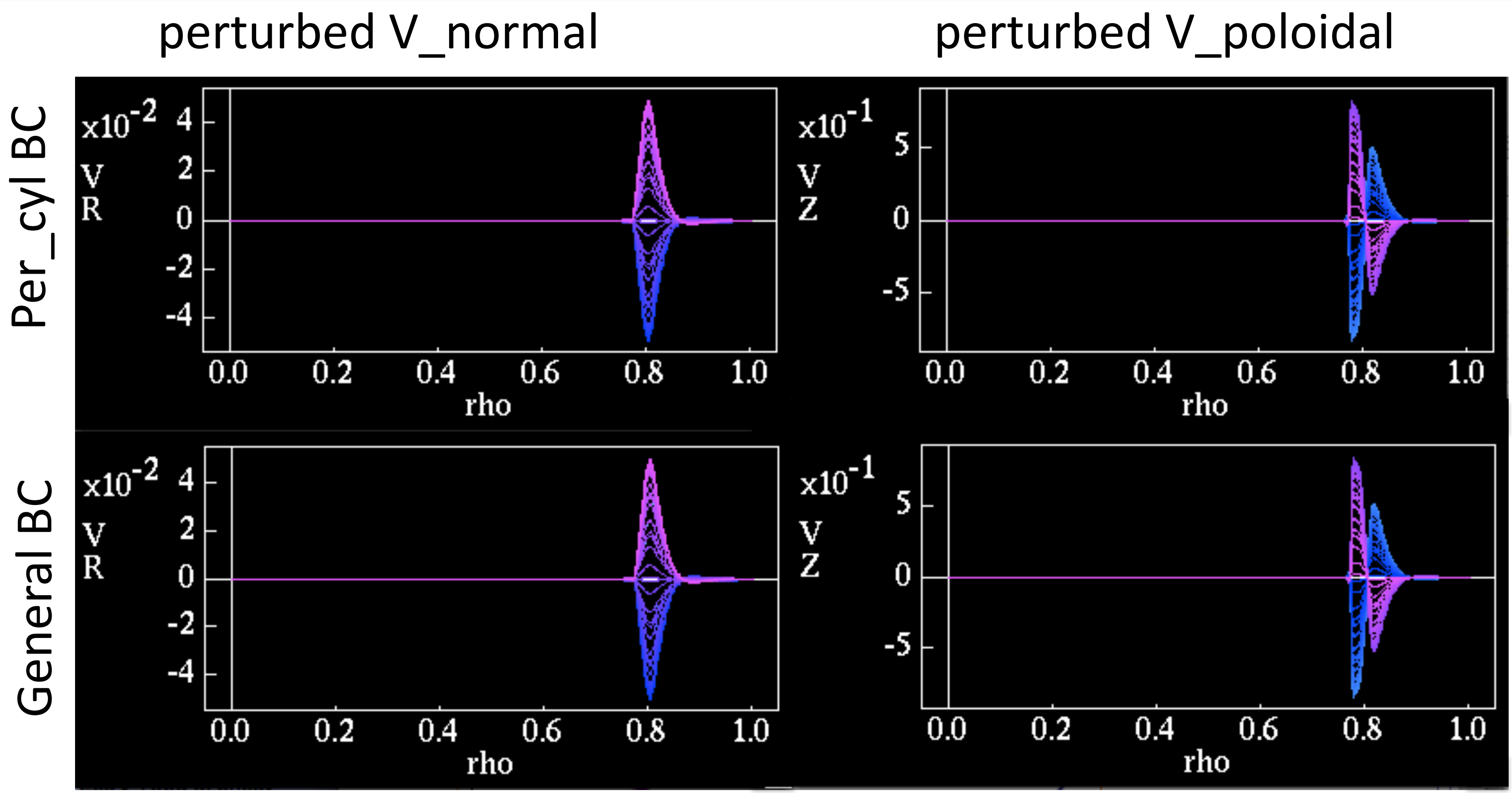

- Spike in velocity profile is due to the plasma column kinking into the vacuum-like region between it and the wall.

Conclusions

- A full resistive wall boundary condition that can be used for toroidal and cylindrical geometries with coupled m numbers has now been implemented in NIMROD.
- This generalized boundary condition has been tested against theory and previous numerical work for the specific case of a periodic cylinder, matching analytic growth rates for the RWM to within 3% error.
- Generalized boundary conditions can be used with the analytic vacuum response matrix for a periodic cylinder to study non-linear interaction of modes with the RW and each other in a cylinder.

Future Work

- Examine non-linear evolution of tearing modes with different m numbers as they interact with each other and the wall (for a periodic cylinder).
- Consider how to handle n=0 component of the electric field in the RW for shots with changing plasma current.
- Implement toroidal vacuum response matrix (calculated by GRIN).
- Use realistic equilibria and walls to study experimentally relevant cases:
  - ITER-like wall and RWM unstable equilibrium + rotation?
  - NSTX-like wall to reproduce VDEs, compare to M3D code
- Consider the addition of external (to the wall) RMPs or error fields.